Mechanical-electrical Optoisolator Transducer with current-to-frequency Conversion

Ioan Marcel CIURUŞ[1], Mihai DIMIAN[2], Adrian GRAUR[3]
[1,2,3]*Ştefan cel Mare University of Suceava, Romania*
str.Universitatii nr.13, RO-720229 Suceava
[1]*marcelciurus@usv.ro,* [2]*dimian@eed.usv.ro,* [3]*adrian.graur@usv.ro*

***Abstract* — A novel design for a mechanical-electrical transducer is presented in this article along with the preliminary testing of the transducer prototype. By using a Polaroid optocoupler as the motion sensor, this device combines the transducer feature to convert mechanical signals to electrical ones with the optoisolator feature of galvanic separation between two voltage modules. Signal conditioning circuit is a current-to-frequency converter, while the obtained signals are logically compatible and can be processed by a microprocessor. The device is aimed for application in the areas of automation and mechatronics.**

Index Terms — Current-to-frequency conversion, Optical polarization, Optoelectronics, Polaroid optocoupler, Transducer

I. INTRODUCTION

One of the present demands in the development of industrial processes is the rigorous control of the parameters for different components of the machine-tools and industrial robots [1]. The precise determination of the component position, speed, and acceleration requires multi-disciplinary approaches which combine fine mechanics, electronics and information technology [2].

This article presents a novel design for a mechanical-electrical transducer based on a Polaroid optocoupler as the motion sensor. As photoelectrical conversions eliminate the influence of electromagnetic disturbances [3], this device combines the transducer feature to convert mechanical signals to electrical ones with the optoisolator feature of galvanic separation between two voltage modules. The originality of our approach consists of replacing the disk or disks having transparent and opaque spaces, which are usually used in such devices for controlling the light beam, with a system of Polaroid filters (analyzer, polarizer) leading to novel optoisolator coined as Polaroid optocoupler [4]. The Polaroid optocoupler can command both digital and analog integrated circuits can be better miniaturized than optical transducers with disks.

When the Polaroid optocoupler sends data to a microprocessor, the optocoupler output driver can be an analog-to-digital converter [5]. However the focus of this paper is on current-to-frequency converter since the rigorous knowledge of the movement parameters for the components of a machine-tool requires a conversion with a large number of bits. The rectangular impulses generated by this driver can be counted with a microprocessor internal counter.

II. PROPOSED SCHEME

The block diagram of the mechanical-electrical optoisolator transducer has the following parts: the driver of the transmitter module (T_x) of the Polaroid optocoupler, the Polaroid optocoupler LED-phototransistor and the driver of the receiver module (R_x), which are represented in Fig.1.

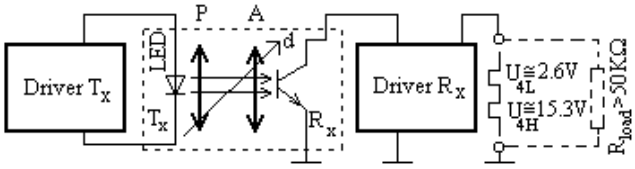

Figure 1. The block diagram of the mechanical-electrical optoisolator transducer with current-to-frequency conversion.

The corresponding schematic diagram is presented in Fig. 2. The driver of (T_x) module is an independent current source, while the light source of the Polaroid optocoupler is a super bright white LED with the luminous intensity on the direction of the longitudinal axis of (10365±226) mcd for a 19mA current, where the current intensity is regulated with the linear P_1 potentiometer. A rotating P-polarizer Polaroid filter is attached to LED optical output and a fixed A–analyzer Polaroid filter is attached to the photoreceiver optical input, both filters having a thickness of 0.7mm. A mechanical system is used for the axial assembly and the rotation/translation movement of these components.

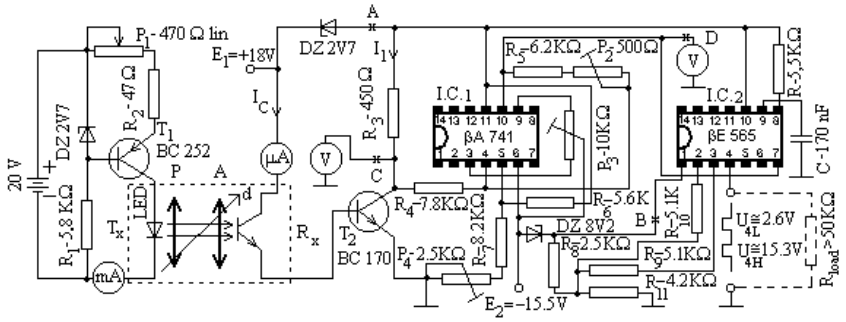

Figure 2. The schematic diagram of the mechanical-electrical optoisolator transducer with current-to-frequency conversion.

The optocoupler's photosensitive detector is a BPV11 silicone NPN Phototransistor [6] which functions under conditions of open base circuit**,** having the emitter-collector voltage of 18V. The driver of the (R_x) module of the Polaroid optocoupler is a current-to-frequency converter. This driver's T_2-BC170 transistor has the function of converting the current intensity (I_C) through the phototransistor into voltage. The domain of (V_C) voltage in which (I_C) current is converted differs from that of the command (V_D) voltage of the integrated circuits I.C.$_2$-βE565. For conversion $V_C \rightarrow V_D$, the operational amplifier I.C.$_1$-βA741 is used.

I.C.2 is a phase locked loop (PLL). Among the functional blocks of the PLL (βE565), we only used the voltage-controlled oscillator (VCO) in order to make the voltage-frequency conversion.

III. EXPERIMENTAL RESULTS

In Table I, the measured values of electric current intensities (I_C) are presented for selected values of angle (α) between the polarizing planes of the two filters and distance (d) between (T_x) and (R_x) modules. The transfer characteristics families of the LED-phototransistor Polaroid optocoupler, $I=I(\alpha)_{d=const.}$ and $I=I(d)_{\alpha=const.}$, are plotted in Fig. 3 and Fig. 4, respectively.

TABLE I. THE OUTPUT ELECTRIC CURRENT INTENSITIES OF THE LED–PHOTOTRANSISTOR POLAROID OPTOCOUPLER EXPRESSED IN (MA), FOR DIFFERENT VALUES OF ANGLE (A) BETWEEN POLARIZING (P) AND (A) PLANES AND OF THE DISTANCE (D) BETWEEN (T_x) AND (R_x) MODULES.

α	d (mm)					
(DEG)	78	84	94	102	114	124
0	89	78	62	52.5	42	36
10	86	76	60	50	40	35
20	79	69	55	46	37	31
30	67	59	47	39	31	27
40	54	47	37	31	25	21
50	40	35	27	23	18	15.5
60	27	23	17	14	12	9.5
70	15	12.5	9	8	6.5	5
80	8.5	7	5.5	4.5	3.5	2.5
90	5	4	3.5	3	2.5	2

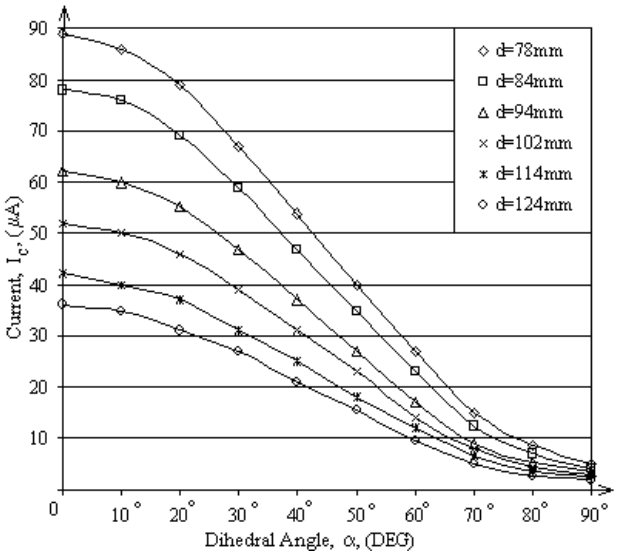

Figure 3. The transfer characteristics family $I_C=I_C(\alpha)_{d=const.}$ of the LED–phototransistor Polaroid optocoupler.

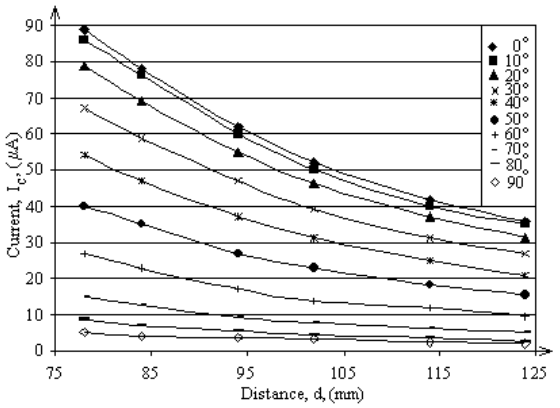

Figure 4. The transfer characteristics family $I_C=I_C(d)_{\alpha=const.}$ of the LED–phototransistor Polaroid optocoupler.

In order to quickly and accurately determine the movement parameters for different components of a machine-tool, the extreme values of the (I_C) current need to be known with high precision. This involves a precise knowledge of the extreme values taken by (α) and (d) [7]. Otherwise, the polarizing voltage of the T_2 transistor junctions could be inaccurately computed, and consequently, the transfer characteristic $V_C=V_C(I_C)$ of the current-to-voltage converter could be diverted from the linear form. For the analysis of these processes, the domain of the values of distance (d) is a little larger than the one for which the driver of the (R_x) module was designed.

In Table II are rendered the values of (V_C) voltage corresponding to the (I_C) currents from Table I. Voltage (V_C) is measured between the collector and the transducer chassis ground. In Fig. 5, the transfer characteristic $V_C=V_C(I_C)$ of the current-to-voltage converter is graphically represented. To make this graphic, were used the values from Tables I and II.

TABLE II. THE VOLTAGE (V_C) EXPRESSED IN (V), FOR DIFFERENT VALUES OF ANGLE (A) AND OF THE DISTANCE (D) BETWEEN (T_x) AND (R_x) MODULES.

α	d (mm)					
(DEG)	78	84	94	102	114	124
0	2.0	2.5	5.0	6.8	8.0	9.0
10	2.0	2.8	5.5	7.0	8.5	9.5
20	2.5	3.5	6.3	7.5	9.5	10.0
30	4.1	5.5	7.5	8.7	10.0	11.0
40	6.5	7.5	9.0	10.0	11.3	11.5
50	8.5	9.5	11.0	12.0	12.5	13.0
60	11.0	11.5	12.5	13.0	13.5	13.5
70	13.0	13.0	14.0	14.3	14.5	14.5
80	14.0	14.3	14.5	14.5	14.7	14.8
90	14.4	14.5	14.7	14.8	14.8	15.0

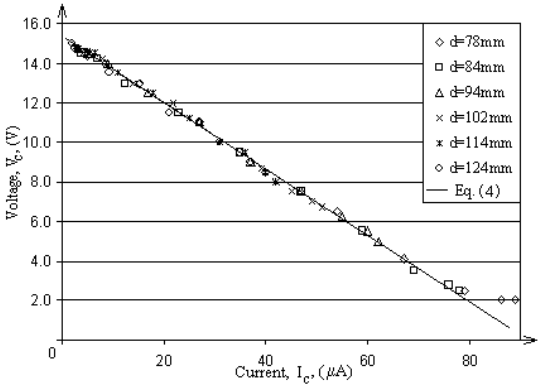

Figure 5. The transfer characteristic $V_C=V_C(I_C)$ of the current-to-voltage converter.

TABLE III. THE VOLTAGE (V_D) EXPRESSED IN (V), FOR DIFFERENT VALUES OF ANGLE (A) AND DISTANCE (D) BETWEEN (T_X) AND (R_X) MODULES.

α	d (mm)					
(DEG)	78	84	94	102	114	124
0	14.9	14.8	13.7	12.6	11.2	10.5
10	14.9	14.8	13.5	12.3	11	10.3
20	14.9	14.7	13	11.8	10.4	9.8
30	14.6	13.5	11.8	10.7	9.5	9
40	12.8	11.9	10.5	9.5	8.5	8.2
50	10.9	10.1	9	8.2	7.5	7.3
60	8.8	8.3	7.6	7.1	6.6	6.5
70	7.2	6.9	6.5	6.2	5.9	5.8
80	6.4	6.2	6	5.8	5.6	5.5
90	6.1	6	5.8	5.7	5.5	5.4

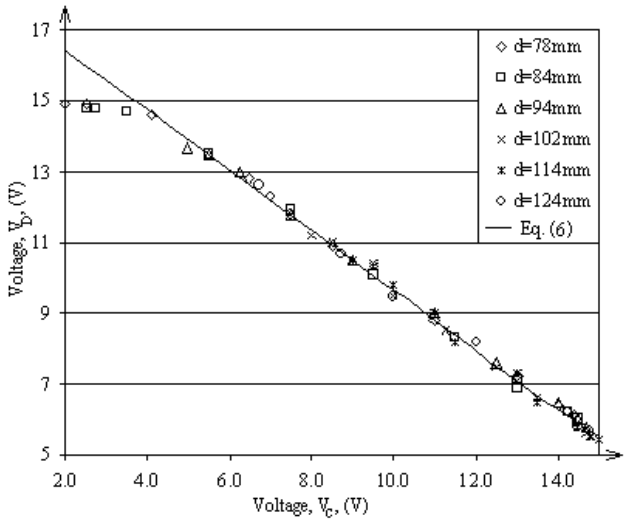

Figure 6. The transfer characteristic $V_D=V_D(V_C)$ of the voltage range converter.

TABLE IV. THE FREQUENCY (F) EXPRESSED IN (HZ), FOR DIFFERENT VALUES OF ANGLE (A) AND DISTANCE (D) BETWEEN (T_X) AND (R_X) MODULES.

α	d (mm)					
(DEG)	78	84	94	102	114	124
0	50	60	180	310	490	580
10	50	60	200	340	500	600
20	50	80	270	410	550	640
30	80	210	400	520	660	710
40	280	390	560	660	760	790
50	490	590	710	790	860	900
60	720	770	870	910	960	980
70	910	930	980	1010	1040	1060
80	1010	1030	1060	1070	1080	1100
90	1050	1070	1090	1090	1100	1110

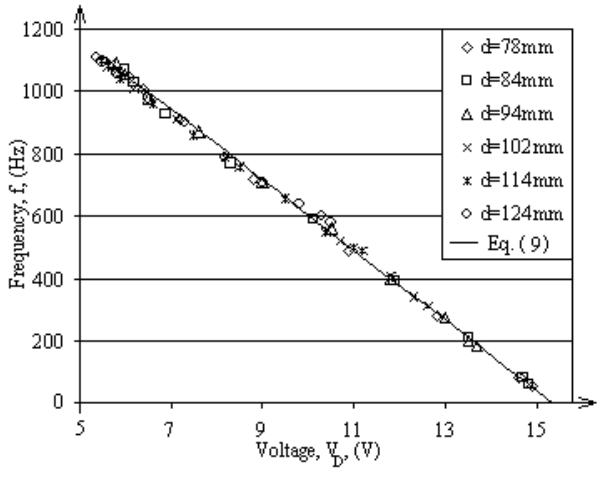

Figure 7. The transfer characteristic $f=f(V_D)$ of the current-to-frequency converter.

The (V_D) values of the voltage obtained by converting the voltage from Table II using $I.C._1$ are shown in Table III. Voltage (V_D) is measured between the 7 pin of the βE565 and the transducer's chassis ground. In Fig. 6, the transfer characteristics of the voltage range converter are presented based on the data from Tables I and III.

In Table IV, there are presented the values of the frequency (f) obtained after the conversion of voltages (V_D) by I.C.2. By graphically representing data from Table III and IV, the transfer characteristic of the voltage-to-frequency converter is obtained, as one can see in Fig.7.

By using data from Tables I and IV, the transfer characteristics families of the mechanical-electrical optoisolator transducer with the current-to-frequency conversion are obtained. $f=f(\alpha)_{d=const.}$ and $f=f(d)_{\alpha=const.}$ are presented in Fig.8 and Fig. 9, respectively.

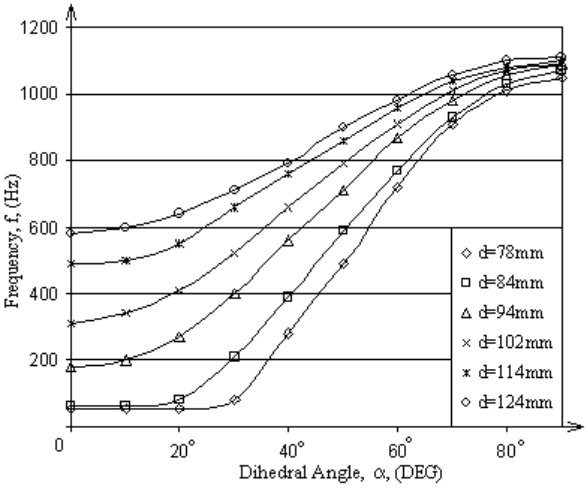

Figure 8. The transfer characteristics family $f=f(\alpha)_{d=const.}$ of the mechanical-electrical optoisolator transducer with the current-to-frequency conversion.

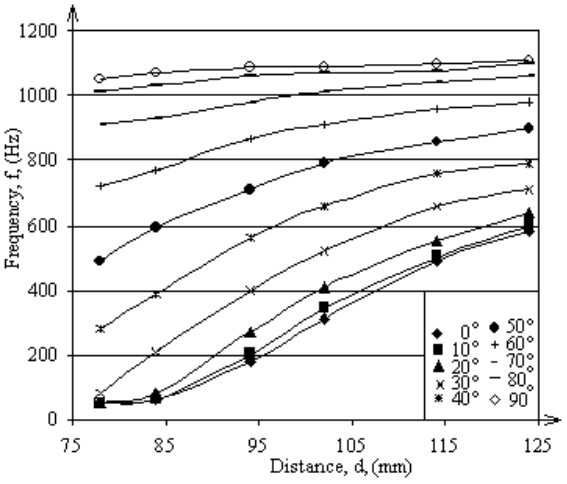

Figure 9. The transfer characteristics family $f=f(d)_{\alpha=const.}$ of the mechanical-electrical optoisolator transducer with the current-to-frequency conversion.

IV. CHARACTERISTICS MODELING

If the intensity of the current through the LED in Fig. 2 is maintained constant then the intensity of the light beam ($\mathcal{I}_o$) incident on the surface of the polarizer filter (P) is constant in time. Knowing that the intensity of the light beam is proportional with the square of the maximum value of the electrical field's intensity, according to Malus's law, one

can show that the dependence of the light beam's intensity ($\mathcal{I}$) at the output of the analyzer filter (A) on the intensity of the light beam incident on the (P) filter, is given by the following relation:

$$\mathcal{I} = \mathcal{I}_0 \cdot \cos^2 \alpha \tag{1}$$

where (α) is the angle between the polarizing plans of the two filters.

In the case of the LED-phototransistor bipolar polaroid optocouplers, the current-illumination relation is a power law with exponent a ≤1. By taking also into account the inverse square distance law relating the detected illumination to the radiation luminous intensity, the dependence of intensity (I_C) of the electric current at the collector on angle (α) and distance (d) between (T_x) and (R_x) modules can be expressed as follows:

$$I_C = k \cdot \frac{\cos^{2a} \alpha + T}{d^{2a}} \tag{2}$$

where k is a proportionality constant specific to the optocoupler. Since the extinction ratio of real polarizer filter is not zero, an additional parameter T was introduced in (2) to account for the transmission of the light beam through the system of Polaroid filters incident in case of extinction (α=90°);

From the light characteristics of the n-p-n, BPV 11 phototransistor used in our experiments power coefficient *a* is found to be equal to 1 when the emitter-collector voltage is 18 V. By using the experimental data from Table I for the extreme cases α=0° and α=90° when d=102mm, the values for the empirical constants (T) and (k) are obtained. As a result, theoretical transfer characteristics (2) for our prototype reads as follows:

$$I_C = 515\text{mA} \cdot \text{mm}^2 \cdot \frac{\cos^2 \alpha + 0.06}{d^2} \tag{3}$$

A comparison between the experimental transfer characteristics family measured for our Polaroid optocoupler prototype (see also Fig. 3) and the theoretical transfer characteristics family given by (3) is presented in Fig. 10. The measurement data are represented by symbols and the theoretical characteristics by continuous lines.

The signal processing of the (R_x) module starts with T_2 transistor which converts (I_C) current into (V_C) voltage. The transfer function of the current-to-voltage converter from Fig. 2 can be expressed as follows:

$$V_C = V_A - \beta_F \cdot R_3 \cdot I_C = (E_1 - 2.7\text{V}) - \beta_F \cdot R_3 \cdot I_C \tag{4}$$

where V_A is the potential at point (A) of the circuit from Fig.2 and β_F is the forward common emitter current gain and is equal to 364 for the transistor used in our device.

The domain of (V_C) voltages is then converted into (V_D) voltages with I.C.$_1$. In the case of operational amplifiers from Fig. 2, the gain of the amplifier is given by.

$$A = \frac{V_D - V_{Dm}}{V_C - V_{CM}} = -\frac{R_5 + R_{P2}}{R_4} \tag{5}$$

where V_{CM} is maximum voltage at the inverting input of I.C.$_1$, V_{Dm} is minimum voltage at the output of I.C.$_1$, and R_{P2} is resistance from the circuit of P_2 potentiometer.

It is apparent from (5) that the expression of the transfer function of the voltage range converter is:

$$V_D = V_{Dm} + \frac{R_5 + R_{P2}}{R_4} \cdot (V_{CM} - V_C) \tag{6}$$

In the case of our prototype:

$$V_{CM} = E_1 - 2.7\text{V} - \beta_F \cdot R_3 \cdot k \cdot \frac{T}{d_M^{2a}} = 15\text{V} \tag{7}$$

and

$$V_{Dm} = \frac{(E_1 - 2.7\text{V}) \cdot (R_7 + R_{P4}) \cdot (R_4 + R_5 + R_{P2})}{(R_6 + R_7 + R_{P4}) \cdot R_4} - \frac{R_5 + R_{P2}}{R_4} \cdot \left(E_1 - 2.7\text{V} - \beta_F \cdot R_3 \cdot k \cdot \frac{T}{d_M^{2a}} \right) = 5.48\text{V} \tag{8}$$

where (d_M) is the maximum distance between (T_x) and (R_x) modules. The resulting theoretical characteristic is plotted in Fig. 6 by continuous line and is in good agreement with the experimental measurements.

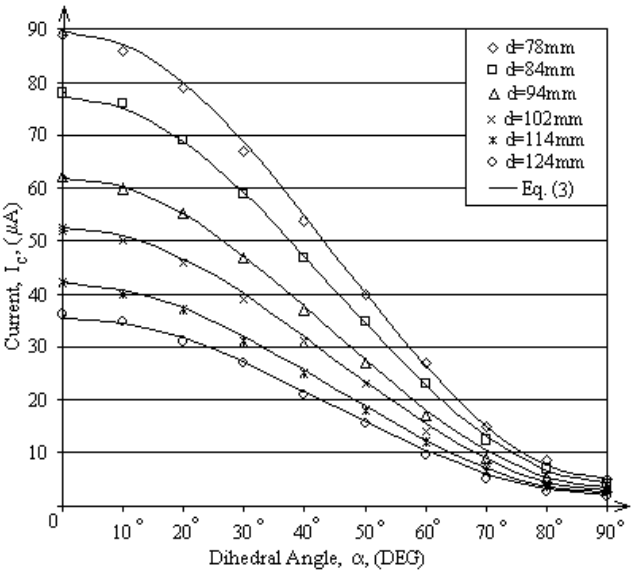

Figure 10. Graphical representation of the theoretical and the experimental characteristics families $I_C=I_C(\alpha)_{d=const.}$ of the LED–phototransistor Polaroid optocoupler.

Next, voltages (V_D) are converted into frequencies by I.C.$_2$. The transfer function of the voltage-to-frequency converter is given by the following relation [9]:

$$f \cong \frac{V_A - V_D}{2 \cdot [0.22 \cdot (V_A - V_B) - 0.3] \cdot R \cdot C} \tag{9}$$

which is represented by continuous line in Fig. 7.

By replacing in (9), the electrical potentials at points A and B with their expression of voltages E_1 and E_2 (see Fig. 2) the expression for frequency becomes:

$$f \cong \frac{E_1 - 2.7\text{V} - V_D}{[0.44 \cdot (E_1 - E_2) - 4.94\text{V}] \cdot R \cdot C} \tag{10}$$

From eqs. (2), (4), (6), (7), (8) and (10), the following expression is derived for the frequency generated by the mechanical-electrical optoisolator transducer with current-to-frequency conversion as a function of the movement parameters (α) and (d):

$$f(\alpha,d)\cong\frac{(E_1-2.7V)\cdot\left(1-\frac{1}{R_4}\cdot\left[\frac{(R_7+R_{P4})\cdot(R_4+R_5+R_{P2})}{R_6+R_7+R_{P4}}-R_5-R_{P2}\right]\right)-\frac{\beta_F\cdot k\cdot R_3(R_5+R_{P2})}{R_4}\cdot\frac{\cos^{2a}\alpha+T}{d^{2a}}}{[0.44\cdot(E_1-E_2)-4.94V]\cdot R\cdot C}\quad(11)$$

In Fig.11 and Fig.12, the families of theoretical characteristics $f=f(\alpha)_{d=const.}$ and $f=f(d)_{\alpha=const.}$ computed by using (11) are plotted against the experimental transfer characteristics of our prototype for the optoisolator transducer with current-to-frequency. The theoretical curves are represented by lines while the experimental data, which were also given in Figs. 8 and 9, are plotted as symbols.

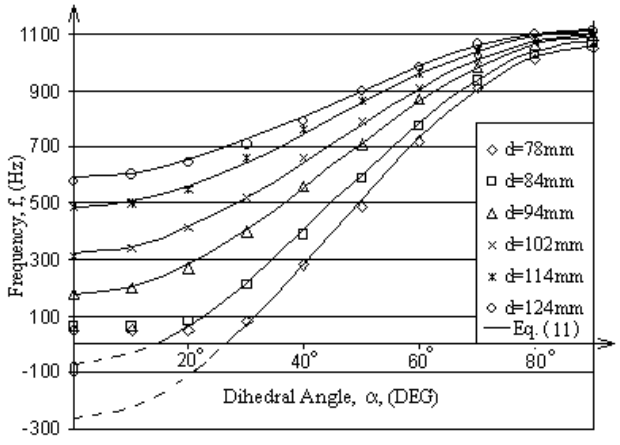

Figure 11. Graphical representation of the theoretical and the experimental characteristics families $f=f(\alpha)_{d=const.}$ of the mechanical-electrical optoisolator transducer with the current-to-frequency conversion.

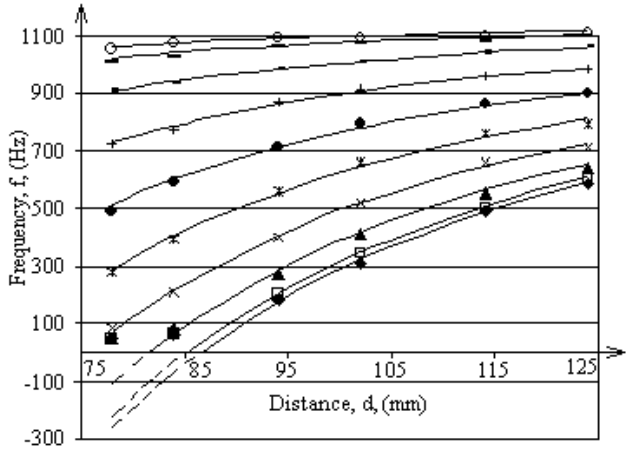

Figure 12. Graphical representation of the theoretical and the experimental characteristics families $f=f(d)_{\alpha=const.}$ of the mechanical-electrical optoisolator transducer with the current-to-frequency conversion.

Although the expression (11) can be mathematically extended in the field of negative frequencies, as can also be seen from the previous Figures, the representations in this area do not actually have a physical meaning.

A general view over the deformation of the experimental family characteristics f=f(d, α) because of the saturation effect, emerging for small values of the (α) and (d) movement parameters, can be noticed in the 3D representation from Fig.13.

V. ANALYSIS OF BORDELINE CASES

The role of position and movement transducers is to quickly and precisely determine the positions of movement parameters of some components of different mechanisms.

In the case of the transducer presented in this paper, the determination is possible when function (11) rigorously describes the real movement of the (Tx) module as compared to (Rx) module.

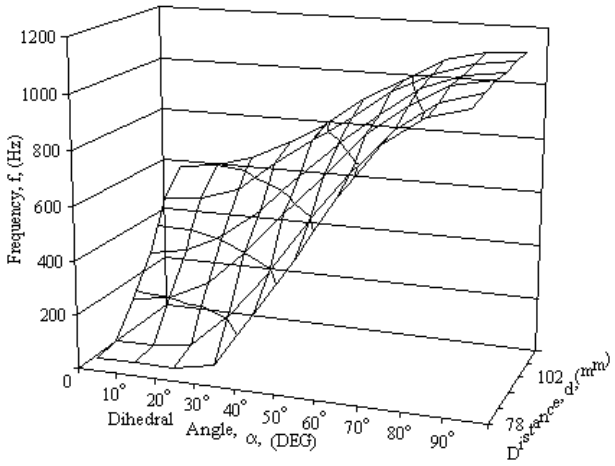

Figure 13. 3 D graphical representation of the experimental characteristics families f=f(α,d) of the mechanical-electrical optoisolator transducer with the current-to-frequency conversion.

This involves accurate knowledge of the extreme values that can be taken by (α) and (d) measures as well as the form of function (2).

In order to analyze these processes, the domain of the values of distance (d) is a little bit higher than that for which the driver of the (R_x) module was designed.

When the distance (d) between (T_x) and (R_x) modules is smaller than that one for which the transducer's driver was designed, for small values of (α) angle the current through the phototransistor (I_C) increases to the maximum admitted value. This increase brings the operation of the phototransistor (T_2) in the neighborhood of the saturation area. In this case, the transfer characteristic $I_{C2}=I_{C2}(I_{B2})_{Vc=const.}=I_1(I_C)_{Vc=const.}$ becomes nonlinear.

This phenomenon can be noticed in the following cases: d=84mm for α=0° and d=78mm for $\alpha\in[0°, 20°]$, Table II.

The nonlinearity characteristic $I_1=I_1(I_C)_{VC=CONST.}$ determines the lack of linearity in the inferior part of the transfer characteristic $V_C=V_C(I_C)$ of the current voltage-to-voltage converter, Fig.5.

At the same time, too big values of the (I_C) current, determines the entrance of the operational amplifier in the saturation area for small values of the input voltages which results in large values of the output voltages Fig.6. In this region, the transfer characteristic of the voltage converter becomes nonlinear.

This saturation effect can be also found in the case of the current-to-frequency converter for small values of the frequencies generated by the VCO module of I.C.$_2$., Fig. 8, 9, 13.

Because of this effect, it is impossible for the transducer to perceive the modification of distance (d) and the (α) angle in the case of exceeding border values. Consequently,

the movements of the component parts of the machine-tools will receive erroneous commands.

Another borderline case is met when currents intensities become too small. This situation can be encountered if the values of (α) and (d) parameters become too big. In these conditions, the VCO module of I.C.$_2$ becomes unstable, generating a signal characterized by frequency leaps. At the same time, although the amplitude of the signal doesn't change, a considerable modification of the offset current appears as seen in Fig. 14 and 15.

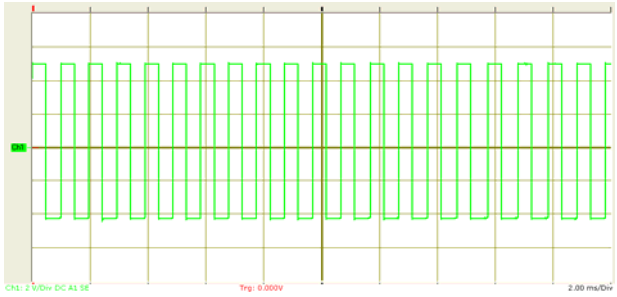

Figure 14. The shape of the signal emitted by the transducer, for a command current of the driver (R_x) found at the inferior border of the domain (I_C=6.5 μA).

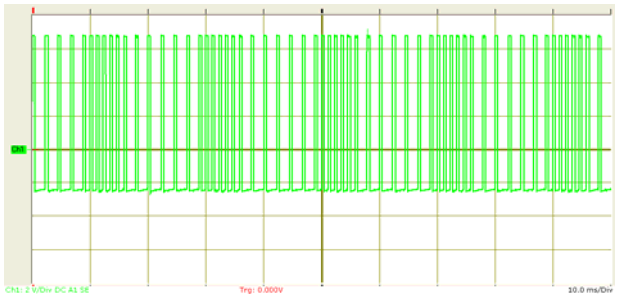

Figure 15. The shape of the signal emitted by the transducer, for a command current of the driver (R_x) found under the inferior border of the domain (I_C=6.5 μA).

This instability of VCO module will determine the chaotic commanding of the machine-tools' component parts.

VI. CONCLUSIONS

The transducer proposed by us, using a Polaroid optocoupler sensor is not affected by electromagnetic disturbance. This sensor can be better miniaturized than optical sensors equipped with disk/disks with transparent and opaque areas. The electrical signals generated by the proposed transducer are analog signals and contains more information than the signals emitted by optical sensors disk/disks.

Signal conditioning circuit of the transducer is not a classic analog-to-digital converter. Its conversion rate is lower than a parallel analog-to-digital converter.

Although slower, the proposed current-to-frequency converter allows the conversion of a large number of bits on the output signal of the sensor. This conversion has the advantage to specify strict parameters of the components of machine-tools.

Optical sensors disk/disks may work in binary code, decimal code or Gray code. The code is required by way of realization of the disc.

If the signal conditioning circuit is a classic analog-to-digital converter it imposes the type of coding scheme of the transducer.

By using the proposed current-to-frequency converter, the transducer can work with any of the three codes. In this case, the type of code will be determined by the numerator processor. Due to the fact that this transducer does not require the use of a processor to decode a specific code, it offers the user a great freedom in designing the system of command and control of machine tools.

Transducer's frequency output signal contains information related to the value of the (α) and (d) movement parameters.

The maximum frequency which can be generated by the VCO module of βE565 is fM=500 KHz and the minimum frequency accomplishes the condition fm ≥ fM/22 [9]. These characteristics of I.C.2., allow the obtaining of some high resolution transducers.

The signal generated at the transducer's output is a function of f=f(d,α) type (11). Such a signal permits microprocessors to obtain complex information concerning the position, the movement direction, the speed and the acceleration of the component parts of the machine-tools.

The transducer presented in this article functions for angles whose value is comprised in α ∈[0°, 90°] domain.

This thing restricts the rotation movements of an engine to a certain number of revolutions. The number of revolutions depends on the domain in which the (α) angle can take values and on the characteristics of the mechanical system used at gearing down the rotation movement.

The modification of distance (d) between the two modules can be also used to compensate the effects that appear because of LED ageing which is a part of the optocoupler.

The optocoupler's internal structure allows for its miniaturization.

These transducers are generally aimed at automation and mechatronics applications.

REFERENCES

[1] J. Corda and J.K. Al-Tayie, "Enhanced performance variable-reluctance transducer for linear-position sensing", IEE Proc. Electric Power Applications, vol. 150, pp. 623-628, Sept. 2003.

[2] A. Drumea, A. Vasile, P. Svasta and I. Ilie, "Modelling and simulation of simple mechatronic system - position control solution based on linear variable inductor displacement transducer", Proc. IEEE 2nd Electronics System-Integration Technology Conf., Greenwich, GB, Sept. 2008, pp. 225 – 230.

[3] K. Tsubata, K. Suzuki, S. Mikami and E.I. Osawa, "Recognition of lawn information for mowing robots", Proc. IEEE 4th Int. Conf. Autonomous Robots and Agents, Wellington, NZ, Feb. 2009, pp.15-20.

[4] I.M. Ciuruş, "Optocuplor polaroid" (patent pending), OSIM Bucureşti, RO, a2009 00270, 2009.

[5] D.A. Rauth and V.T. Randal, "Analog-to-digital conversion. part 5", IEEE Instrumentation & Measurement Magazine, vol. 8, pp. 44-54, Oct. 2005.

[6] http://www.vishay.com/docs/81504/81504.pdf.

[7] S. Brock and J. Deskur, "The problem of measurement and control of speed in a drive with an inaccurate measuring position transducer", Proc. IEEE 10th Int. Workshop on Advanced Motion Control, Trento, IT, March 2008, pp. 132-136.

[8] I.M. Ciuruş, "LED-Photoresistor Polaroid Optocouplers", Proc. 3rd Int. Symp. Electrical Engineering and Energy Converters, Suceava, RO, Sept. 2009, pp. 257-262.

[9] M. Ciugudean et al., "Circuite integrate liniare. Aplicații", Editura Facla, Timişoara, RO, 1986, ch. 7, sec. 7.2, pp. 218-227.